

A Small Molecule That Binds and Inhibits the ETV1 Transcription Factor Oncoprotein

Marius S. Pop^{1,2}, Nicolas Stransky², Colin W. Garvie², Jean-Philippe Theurillat^{1,2}, Emily C. Hartman², Timothy A. Lewis², Cheng Zhong², Elizabeth K. Culyba², Fallon Lin³, Douglas S. Daniels², Raymond Pagliarini³, Lucienne Ronco², Angela N. Koehler^{2,4,5}, and Levi A. Garraway^{1,2}

Abstract

Members of the ETS transcription factor family have been implicated in several cancers, where they are often dysregulated by genomic derangement. ETS variant 1 (*ETV1*) is an ETS factor gene that undergoes chromosomal translocation in prostate cancers and Ewing sarcomas, amplification in melanomas, and lineage dysregulation in gastrointestinal stromal tumors. Pharmacologic perturbation of *ETV1* would be appealing in these cancers; however, oncogenic transcription factors are often deemed "undruggable" by conventional methods. Here, we used small-molecule microarray screens to identify and characterize drug-like compounds that modulate the biologic function of *ETV1*. We identified the 1,3,5-triazine small molecule BRD32048 as a top candidate *ETV1* perturbation. BRD32048 binds *ETV1* directly, modulating both *ETV1*-mediated transcriptional activity and invasion of *ETV1*-driven cancer cells. Moreover, BRD32048 inhibits p300-dependent acetylation of *ETV1*, thereby promoting its degradation. These results point to a new avenue for pharmacologic *ETV1* inhibition and may inform a general means to discover small molecule perturbation of transcription factor oncoproteins. *Mol Cancer Ther*; 13(6); 1492–502. ©2014 AACR.

Introduction

ETV1 is an oncogenic transcription factor that lacks an enzymatic activity and therefore is deemed "undruggable" by conventional means (1). A significant proportion of the "undruggable" oncoproteins are transcription factors that become deregulated by various somatic genetic events, including gene amplification or balanced translocation (2, 3). The ETS transcription factor family includes several well-known oncogenes affected by genetic aberrations across multiple tumor types (4). For example, 80% of Ewing sarcomas (5) harbor *FLI1* (ETS factor) translocations and a majority of prostate cancers harbor chromosomal translocations of the *ERG* (V-Ets Erythroblastosis Virus E26 Oncogene Homolog Avian), *ETV1* and *ETV4* (ETS variant 4) ETS factor genes (6). In prostate cancer, these translocations arise in the setting of chromoplexy (7) and yield fusion genes involving androgen-regulated

upstream partners such as *TMPRSS2* (transmembrane protease, serine 2) or housekeeping genes (8, 9).

ETV1 is an ETS transcription factor oncogene that is altered in several cancers. Translocations are observed in Ewing sarcoma and prostate cancer, amplification occurs in melanoma (10), and oncogenic lineage dysregulation seems ubiquitous in gastrointestinal stromal tumors (11). These genetic events induce aberrant activation of transcriptional programs that govern various aspects of tumorigenesis (12, 13). *ETV1* is phosphorylated downstream of mitogen-activated protein kinase (MAPK) signaling (14), which enhances its protein stability (15). In addition, the histone acetyltransferase (HAT) p300 (E1A binding protein p300) binds and acetylates *ETV1* at lysines 33 and 116 (16), with both events leading to increased protein half-life and enhanced transcriptional activity (17, 18). A putative "degron" sequence in the N-terminal region of *ETV1* may control its COP1-dependent, proteasome-mediated degradation (19, 20).

In recent years, several small molecules that bind and inhibit regulators of oncogenic transcription factors have been reported. The identification of JQ-1 as a bromodomain perturbation is exemplary in this regard (21). Research to develop tool compounds that interfere with oncogenic ETS factors led to the discovery of YK-4-279, which modulates several ETS family members including *ERG*, *ETV1*, and *FLI1* (22, 23). However, much more work is needed to develop systematic approaches to identify small-molecule "perturbagens" of oncogene transcription factors in general and ETS factors in particular.

Authors' Affiliations: ¹Dana Farber Cancer Institute, Boston; ²Broad Institute; ³Novartis Institute for Biomedical Research; ⁴Department of Biological Engineering; and ⁵Koch Institute for Integrative Cancer Research, MIT, Cambridge, Massachusetts

Note: Supplementary data for this article are available at Molecular Cancer Therapeutics Online (<http://mct.aacrjournals.org/>).

Current address for N. Stransky: Blueprint Medicines, Cambridge, Massachusetts.

Corresponding Author: Levi A. Garraway, Dana-Farber Cancer Institute, 450 Brookline Avenue, D1542, Boston, MA 02115-6048. Phone: 617-632-6689; Fax: 617-582-7880; E-mail: levi_garraway@dfci.harvard.edu

doi: 10.1158/1535-7163.MCT-13-0689

©2014 American Association for Cancer Research.

Small molecule microarray (SMM) screening has been described as a high-throughput means to interrogate many thousands of diverse chemical species for their ability to bind various types of proteins (24). As such, we sought to use SMMs to identify putative ETV1-binding compounds. We reasoned that a subset of such compounds might also inhibit its function and thereby provide new insights into pharmacologic perturbation of these and other transcription factor oncoproteins. These efforts identified BRD32048, a compound that binds ETV1 directly *in vitro* and inhibits its transcriptional activity through a mechanism that involves altered acetylation and compound-induced ETV1 degradation. These results provide new insights into mechanisms that suppress ETV1 activity and may provide a generalizable approach to identify chemical probes of traditionally "undruggable" protein targets.

Materials and Methods

SMM screening

Each SMM slide contained approximately 10,800 printed features including 9,000 unique compounds and was prepared as described previously (25). In total 45,000 compounds were screened. The collection contained commercially available natural products, FDA-approved drugs, known bioactive small molecules, and products of diversity-oriented synthesis (24, 26–28). Each sample was screened against 3 replicate SMMs. Lysates were prepared from HEK293T cells overexpressing HA-tagged ETV1 or vector alone as control. Cells were lysed in mild phosphatase buffer (MIPP) lysis buffer (20 mmol/L NaH₂PO₄, pH 7.2, 1 mmol/L Na₃VO₄, 5 mmol/L NaF, 25 mmol/L β-glycerophosphate, 2 mmol/L EGTA, 2 mmol/L EDTA, 1 mmol/L DTT, 0.5% Triton X-100, complete protease inhibitors). The concentration of total protein was adjusted to 0.3 mg/mL, where ETV1 protein was at approximately 0.5 μg/mL lysate, estimation obtained by comparing Western blot signals of lysates and known amounts of purified ETV1. Each slide was incubated with 3 mL of adjusted lysate for 1 hour at 4°C followed by anti-HA mouse monoclonal (Covance) at 1:1,000 for 1 hour at 4°C in PBS-T buffer (1× PBS, 0.1% Tween-20) supplemented with 0.5% (w/v) BSA. A Cy5-labeled anti-mouse secondary antibody (Millipore) for detection was incubated at 1:1,000 using the same conditions. Each incubation step was followed by 3 washes in PBS-T. Finally, the slides were briefly rinsed in distilled water and spin-dried (26). The slides were immediately scanned using a GenePix 4000B fluorescence scanner (Molecular Devices). The image was analyzed using GenePix Pro software (Axon Instruments) and the raw data were analyzed based on the signal-to-noise ratio and reproducibility. For each feature a CompositeZ score was calculated as described previously (29, 30). The refined data were visualized using Spotfire software (Spotfire TIBCO Software). Assay positives with a composite Z score ≥3 were compared with the control screen and all other SMM screens within ChemBank database to filter nonspecific binders.

Reporter assay

The MMP1 promoter region (1,537 bases upstream of the start codon) was amplified from genomic DNA (5': CTAGCGCAAACCTGATACAGTGGGAAAGGTGG and 3': ATCTCGAGCAGTGCAAGGTAAGTGATGGCT-TCC) and cloned in pGL3 vector (Promega). The tyrosinase promoter region (712 bases upstream of the start codon) was amplified from genomic DNA (5': CTAGCGCTCTTAAACGTGAGATATCCCCACAATG and 3': ATCTCGAGCTTCTCTAGTCTCACAAGGTCTG-CAGG). 501mel cells were seeded in 6-cm Petri dishes and cotransfected with Renilla plasmid (Promega), reporter construct in the presence or absence of ETV1 plasmid. The ratio of reporter to driver was 2:1. After 24 hours, the cells were reseeded in triplicate 96-well plates (~5,000 cells/well) and incubated for 24 hours in the presence of 10 μmol/L BRD32048. The luciferase signal was measured using a dual-luciferase reporter assay (Promega) according to manufacturer's protocol. The luminescence signal was read using a Luminoskan Ascent instrument (Thermo Electron).

Protein purification

A codon-optimized sequence of full-length ETV1 was cloned into a pcDNA3.4 vector (Invitrogen). Synthesized ETV1 sequence included at C-terminus a FLAG tag sequence and a streptavidin binding peptide sequence (SBP tag). The vector was transfected into HEK293F (Invitrogen) cells adapted to grow in suspension to enable the up scaling of protein production. After 72 hours, the cells were harvested and lysed in 1× RIPA buffer supplemented with 2× complete protease inhibitors (Roche). The lysates were cleared by centrifugation at 15,000 rpm for 20 minutes at 4°C and filtered through a 0.2-μm filter. The ETV1 protein was bound to a streptavidin column via SBP tag and eluted in 2 mmol/L biotin in PBS buffer.

Surface plasmon resonance experiments

The surface plasmon resonance (SPR) assays were conducted on a Biacore T200 instrument using Biacore CM5 sensor chips (Biacore). Ethanolamine, *N*-ethyl-*N'*-(3-dimethylaminopropyl) carbodiimide (EDC), *N*-hydroxysuccinimide (NHS), and P-20 surfactant were all obtained from GE Lifesciences. M2 Flag antibody was obtained from Sigma. Reference proteins were obtained from Origene.

Sensor chip preparation. The surface of the sensor chip was conditioned using alternating 1-minute injections (30 μL/min flow rate) of 10 mmol/L glycine pH 2.2 and 50 mmol/L NaOH (repeated 3 times). Surface carboxyl groups were activated with 1:1 0.4 M EDC/0.1 M NHS. A 30 μg/mL solution of anti-FLAG in acetate buffer pH 4.5 was flowed for 10 minutes at a rate of 5 μL/min over all 4 flow cells. The remaining NHS-ester groups on the sensor surface were quenched with a 7-minute injection of 1 M ethanolamine. Recombinant ETV1-FLAG and FLAG-tagged proteins were diluted to 5 μg/mL and captured on the anti-FLAG antibody surface with a 10 to

30 minutes injection at 5 $\mu\text{L}/\text{min}$. Between 1,700 and 2,300 response units (RU) of protein were captured for each assay. The running buffer used during immobilization and capture was HEPES buffered saline (HBS), pH 7.4 with 0.05% P-20 surfactant.

Assay parameters. Small-molecule binding assays were performed at 25°C. The running buffer for the binding assays was HBS, pH 7.4 supplemented with 0.05% P-20 surfactant, and 2% DMSO as a cosolvent. Compounds were diluted from 10 mmol/L DMSO stocks in the appropriate concentrations in buffer with the same solvent concentration as the running buffer (2% DMSO). Binding was measured for a range of concentrations (from 0.78 to 50 $\mu\text{mol}/\text{L}$) injected in duplicate. Compound solutions were injected for 60 seconds at a flow rate of 60 $\mu\text{L}/\text{min}$ followed by 120 seconds of buffer only.

Data analysis. Sensorgram data, the equilibrium plot, and the residual plot were analyzed using BiaEvaluation software (GE LifeSciences). Data were reference-subtracted and corrected for variations in solvent concentration. Binding affinity was calculated using kinetic and steady-state analyses. Kinetic analysis was performed using a least squares fit of a Langmuir 1:1 binding model with locally measured R_{max} values. The timing for association phase is adjusted at 2 seconds after the start of injection and 3 seconds before the end of injection. The steady-state affinity constant for each ligand was derived from a plot of R_{eq} against concentration. The plot was then fitted to a general steady-state model. The graphs displaying the binding level to various surfaces (see Supplementary Figs. S2B, S2C, and S2D and S3B, and S3C) were created using the BiaEvaluation software where the cycle number (X -axis) represents the number of injections of buffer or compound solutions.

Gene expression signatures

LNCAp cells were seeded in 6-well plates and induced with 100 ng/mL doxycycline for 4 days. LNCAp shRNA sequences: shETV1-872 = GCATCTCCAAACTCAACTCAT and shETV1-1117 = CGACCCAGTGTATGAACAA. SK-MEL-28 cells were infected with lentivirus encoding 2 different ETV1 shRNAs (shETV1-3 = GACCAGTGTATGAACACAA and shETV1-5 = GAGAGAGATATGTCTACAAGTTT) or sh-GFP for 24 hours followed by 3 days puromycin selection. Both cell lines were treated with 20 $\mu\text{mol}/\text{L}$ BRD32048 for 16 hours. Each condition was performed in triplicate. Total RNA was collected using QIAgen RNA Extraction Kit. mRNA expression data were obtained using Affymetrix HT Human Genome U133A arrays according to the manufacturer's instructions. Gene-centric expression values were obtained using updated Affymetrix probe set definition files (CDF files) based on Entrez Gene (hthgu133ahsentrezg) from Brainarray version 15, which consists in 12,012 unique genes (31). Background correction was accomplished using RMA (Robust Multichip Average) (32) and quantile normalization (33). For each experimental condition, we fitted a linear model using

Linear Models for Microarray Data (LIMMA; ref. 34) and calculated the average fold-change for each gene between that experimental condition and the control. Gene expression signatures were built using a fold-change cutoff of 1.5 and an FDR-adjusted q -value ≤ 0.25 . P values for the significance of the signatures' overlap were calculated using Fisher exact test taking into account the total number of genes measured (12,012). The microarray data (raw data, normalized data and metadata file) are deposited in GEO (accession No. GSE52154).

Invasion and proliferation assays

Cancer cell lines LNCAp, PC3, and SK-MEL-28 were purchased from ATCC. 501mel and primary melanocytes were purchased from Cell Culture Core Facility, Yale University, New Haven, Connecticut. These cell lines were not authenticated in our laboratory. For invasion assays, cells were serum-starved for 24 hours before conducting invasion assays as described previously (35). Briefly, 250,000 cells/well were seeded in Millipore collagen trans-well plates and each condition was carried out in quadruplicates. The relative amounts of invading cells were measured calorimetrically according to the manufacturer protocol using a SpectraMAX 190 instrument (Molecular Devices). Final values were corrected for background signal (empty well). Proliferation assay was performed in 96-well plates where cells were seeded at 3,000 cells/well followed by compound treatment for 4 days. The relative number of cells was quantified using a Cell-Titer-Glo assay (Promega).

Biotin-oligonucleotide precipitation

Cells expressing Flag-HA-tagged ETV1 were lysed in 1 \times RIPA buffer (50 mmol/L Tris-HCl, pH 7.4, 150 mmol/L NaCl, 1% NP-40, 0.1% SDS, 0.5% sodium deoxycholate, complete protease inhibitors) and diluted 1:10 in EMSA buffer (Pierce) to a final volume of 1 mL. Unlabeled or biotin-labeled oligonucleotides (wt—5': biotin-TCTACCAAGACAGGAAAGCACTTTCCTGGAGATTAATC and scrambled—5': AGTCGTCATGCATTAAGCTGTTGTTGAAGAGTGTAC) were added at 5 pmol/reaction. The compound was added during the pull-down reaction at the stated concentrations. The complexes were precipitated for 2 hours at 4°C using streptavidin magnetic beads (Pierce) and washed 3 times with EMSA buffer. The samples were subjected to Western blotting and probed with anti-HA antibody (Covance).

Immunoprecipitations and Western blotting

Cells were lysed in cold lysis buffer [50 mmol/L Tris pH 7.4, 150 mmol/L NaCl, 0.1% (v/v) NP-40, 0.5% (v/v) Triton-100, 5 mmol/L MgCl_2 , 1 mmol/L LM EDTA, 1 \times complete protease inhibitors]. Three milligrams of total protein was subjected to immuno-precipitation using anti-HA agarose beads (Covance) or anti-FLAG M2 agarose beads (Sigma). Samples were washed 3 times in lysis buffer, boiled in 1 \times sample buffer and resolved by SDS-PAGE. p300 silencing was performed using p300 short

hairpin (Santa Cruz) delivered by lentiviral infection. Antibodies used: p300 (N-15; Santa Cruz); P/CAF (C14G9), anti-K-acetyl (Cell Signaling); ETV1 (ab81086, Abcam); vinculin, actin, FLAG (F7425, Sigma); V5 (Invitrogen).

Results

Identification and validation of BRD32048 as direct binder of ETV1

To identify small molecules that interact with ETV1, we pursued an SMM screening approach using methods described previously (25, 26, 36). We used cell lysates instead of purified ETV1 protein for the SMM screens to allow it to undergo additional regulation that might be relevant to the mammalian cellular environment. Like other ETS factors, the ETV1 protein conformation is thought to be regulated by various posttranslational modifications and protein–protein interactions, several of which may be altered during the purification process (25, 26). We generated cell lysates from HEK 293T cells transiently transfected with a HA-tagged ETV1 expression vector resulting in moderate ETV1 expression levels (Supplementary Fig. S1A). A total of 45,000 compounds were screened against HA-ETV1–expressing lysates in triplicate. To identify "hits" from this screen, we calculated a composite Z-score for each compound as published previously (37). Analysis of the composite Z-scores corresponding to the primary SMM screen revealed 6 assay positives (Fig. 1A and Supplementary Fig. S1B) that showed selectivity toward ETV1 relative to >100 additional proteins, including other transcription factors, that had previously been screened using the same SMM library (24, 29).

Next, we sought to determine whether the candidate small-molecule binders identified in the SMM screen might alter ETV1 activity in a cellular context. As a preliminary means to test this, we evaluated the top 6 compounds that emerged from the screen (based on a composite Z-score; see Materials and Methods) in a cell-based reporter construct where the *MMP1* promoter was cloned upstream of the luciferase gene (*MMP1* is a known ETV1 target gene; ref. 17). We consistently observed that compound 1, hereafter termed BRD32048, was able to suppress luciferase activity by ~50% in 501mel melanoma cells, which harbor an *ETV1* amplification (Fig. 1B). To confirm that this molecule did not interfere with the general transcriptional machinery, we also tested its effects in a reporter assay with the tyrosinase (*TYRP1*) promoter, which is activated downstream of the microphthalmia-induced transcription factor (MITF; ref. 38). MITF is a known melanoma oncoprotein (39) that is structurally unrelated to ETS transcription factors. In this context, BRD32048 had no effect on the luciferase signal, suggesting that the compound effects were not solely because of nonspecific transcriptional or posttranscriptional modulation (Supplementary Fig. S1C).

BRD32048 is a substituted [1,3,5]triazine derivative. This synthetic scaffold has previously been observed in orally active PDE inhibitors (40), DHFR inhibitors (41), and PI3K/mTOR inhibitors (42, 43), among others. As an

additional control to rule out nonspecific compound effects, we tested a small set of commercially available BRD32048 analogs that contain the [1,3,5]triazine core but vary either the methoxyphenyl group in the 4-position or the alkyl piperidine group in the 6-position. Using the MMP1 reporter assay in the LNCaP prostate cancer cell line, we observed that major substitutions negatively impacted the inhibitory effect of the triazine scaffold in this reporter assay, whereas minor substitutions failed to enhance its inhibitory activity (Supplementary Fig. S1D). Therefore, we resynthesized BRD32048 and used this compound for all subsequent experiments (the chemical characterization is presented in the Supplementary Material and Methods).

We next sought to determine whether BRD32048 binds ETV1 directly. Here, we used an SPR approach, in which the SPR surface was configured using anti-FLAG M2 antibody to capture FLAG-tagged proteins. The M2 antibody was covalently immobilized to a carboxymethyl dextran surface. Recombinant ETV1 was purified from HEK293F cells (Supplementary Fig. S2A) and captured onto the antibody surface resulting in a stable baseline (Supplementary Fig. S2B). Next, BRD32048 was injected at increasing concentrations from 0.78 to 50 $\mu\text{mol/L}$ (Fig. 1C; see Materials and Methods). For the reference surface we used TBX21, an unrelated transcription factor with a comparable molecular weight (55 kDa) and isoelectric point (~5.8). The reference surface showed no specific interactions, whereas the ETV1 surface recorded an increasing response in a concentration-dependent manner (Supplementary Fig. S2C and S2D).

Kinetic binding analysis of BRD32048 to ETV1 was carried out using a simple 1:1 Langmuir model, which provided a K_D of 17.1 $\mu\text{mol/L}$. The residual plot revealed that the noise level did not exceed 0.4 RU. Moreover, the steady-state equilibrium analysis of the same experiment with TBX21 reference provided a similar K_D of 23.2 $\mu\text{mol/L}$ (Fig. 1C). In addition, the kinetic analysis and steady-state equilibrium analysis using anti-FLAG M2 antibody as reference revealed similar binding affinity for ETV1 (Supplementary Fig. S3A and S3B). We also evaluated binding of BRD32048 to other protein-coated sensor surfaces including RELA, RUNX1, RFDW2, and P/CAF without observing any specific binding (Supplementary Fig. S3C). Moreover, the fact that BRD32048 did not bind to low isoelectric point surfaces (such as TBX21 and RELA) suggests that binding to ETV1 was not merely the result of unspecific charge-based interactions. Together, these results suggested that BRD32048 is capable of binding ETV1 directly.

To confirm that BRD32048 is able to bind ETV1 in lysates, we performed a compound pull-down experiment in which BRD32048 was covalently attached to beads. The coupling was carried out using an isocyanate chemistry-based approach similar to that used in SMM (see Supplementary Methods). Incubation of 501mel cells lysates with BRD32048-beads showed that BRD32048 was able to precipitate endogenous ETV1, whereas addition of

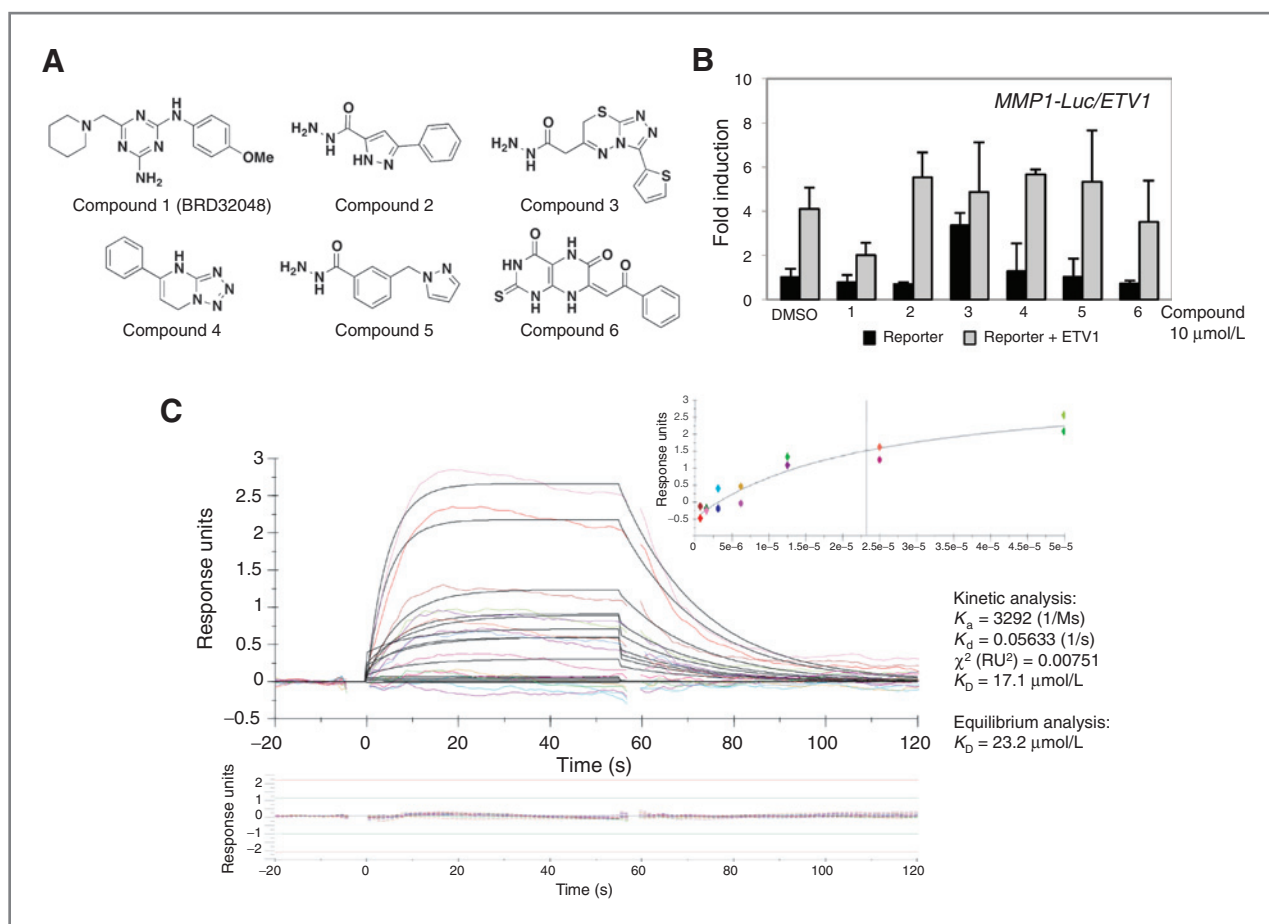


Figure 1. Identification of BRD-K77432048 as a direct ETV1 binder. A, structures for 6 SMM assay positives are shown (see text for details). B, 501mel cells were cotransfected with ETV1- or MMP1-driven firefly luciferase and treated with 10 $\mu\text{mol/L}$ BRD32048 or DMSO for 24 hours. The fold induction of Firefly signals were normalized to Renilla luciferase and divided by the reporter only/DMSO control. C, HEK293F-purified ETV1-FLAG and TBX21-FLAG were captured onto M2 α Flag antibody surface for SPR studies (see text). Compound solution was injected at increasing concentrations from 0.78 to 50 $\mu\text{mol/L}$. RU are corrected for solvent variations and referenced to TBX21 surface. The sensorgram was fitted using a 1:1 Langmuir model and the steady-state equilibrium uses the RU values at 5 seconds before the end of compound injections. Included is the kinetics residual plot as well as the statistical kinetic parameters values for K_a , K_d , and χ^2 .

excess amounts of soluble BRD32048 was able to significantly out compete the immobilized compound from binding to ETV1 (Supplementary Fig. S3D). These data provided further evidence that BRD32048 is capable of binding ETV1 in cells.

BRD32048 modulates an ETV1 transcriptional signature

Although the reporter-based experiments raised the possibility that BRD32048 might perturb ETV1 activity in cells, these assays rely on an artificial read-out that is not necessarily specific to ETV1 function. To ascertain whether BRD32048 might modulate endogenous ETV1 function, we examined its effects on an empirically determined transcriptional signature linked to ETV1 activity. To generate this ETV1 signature, we used derivatives of the LNCaP prostate cancer cell line engineered to express 2 distinct inducible shRNAs against *ETV1* (shETV1-1117 and shETV1-872). LNCaP cells are known to harbor a

chromosomal rearrangement that translocates the entire *ETV1* locus in an androgen-regulated region (8, 9). Induction with doxycycline for 4 days caused a marked reduction of *ETV1* mRNA levels (Fig. 2A), which was also confirmed by quantitative RT-PCR (Supplementary Fig. S4A). The ETV1 protein is virtually eliminated after 4 days of silencing as shown in nuclear extracts (Supplementary Fig. S4B). The proliferation of LNCaP cells also seems to be ETV1 dependent, although the reduction in proliferation only became apparent at later time points (Supplementary Fig. S4C). Using this system, we defined a gene expression signature linked to ETV1 activity by calculating the fold change in expression levels for each gene measured. The final list of differentially expressed genes consist of either upregulated or downregulated genes with a fold change of >1.5.

To derive a gene expression signature linked to BRD32048 exposure, parental LNCaP cells were treated with 20 $\mu\text{mol/L}$ BRD32048 for 16 hours. Using the same

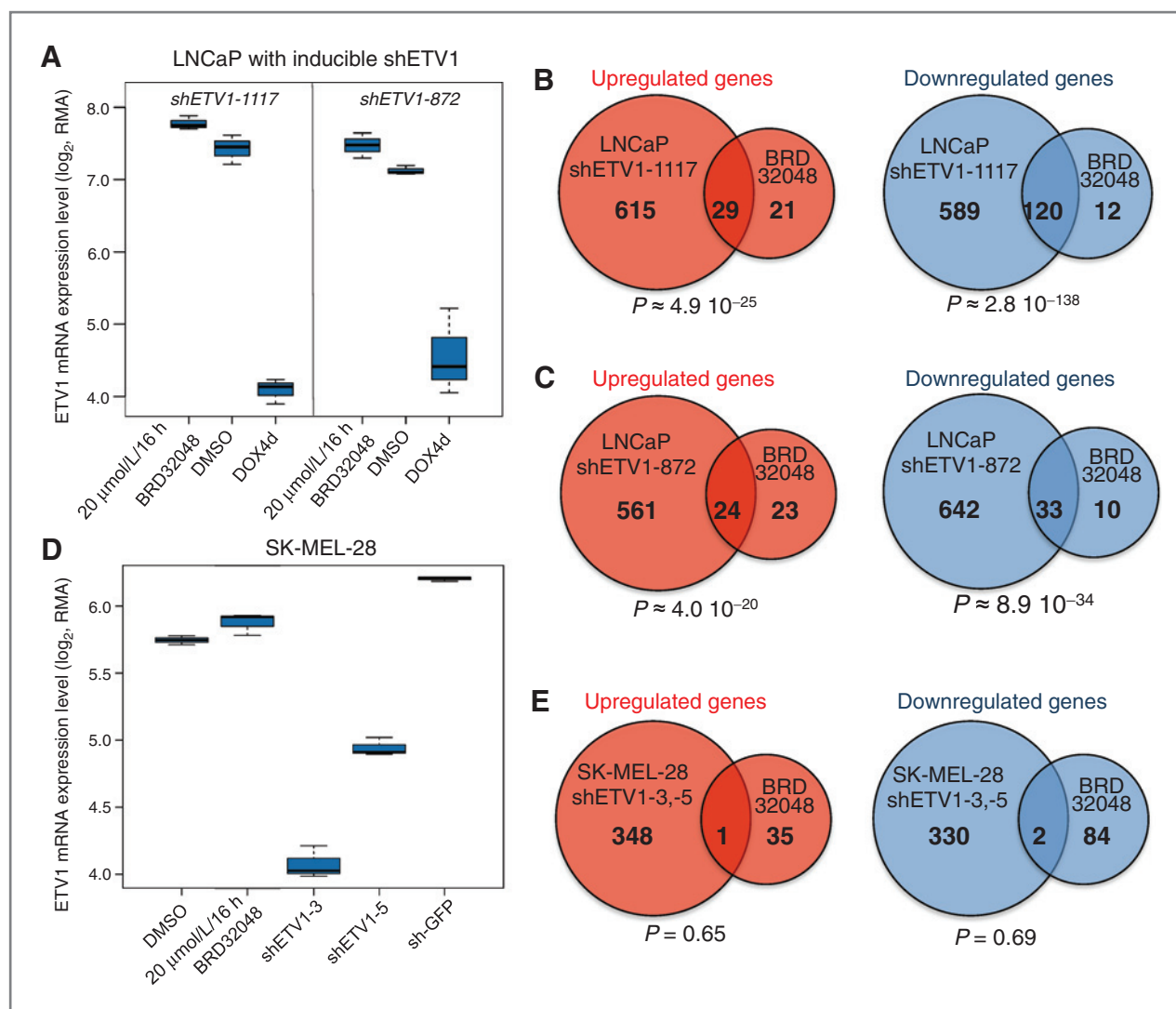


Figure 2. Comparisons between ETV1 and BRD32048 gene expression signatures. A, ETV1 mRNA levels in LNCaP.sh1117 and LNCaP.sh872 cells treated with doxycycline (ETV1 shRNAs), DMSO, or BRD32048. shETV1-induced signature and 20 $\mu\text{mol/L}$ BRD32048-induced signature generated in LNCaP.sh1117 (B) and LNCaP.sh872 (C) are intersected for the upregulated genes and downregulated genes. D, ETV1 mRNA levels in SK-MEL-28 cells expressing shGFP, shETV1-3, or shETV1-5 and treated with DMSO or BRD32048. E, the combined signature induced by shETV1-3 and shETV1-5 was intersected with the 20 $\mu\text{mol/L}$ BRD32048-induced signature for the upregulated genes and downregulated genes. The P value (see Materials and Methods) for each comparison is included.

analysis approach (see Materials and Methods), we identified genes with a fold change greater than 1.5 following BRD32048 exposure, and a false discovery rate of <0.25 . We then determined the overlap between the ETV1 shRNA signature and the BRD32048 signature by intersecting the lists of differentially up- and downregulated genes. Strikingly, $\sim 51\%$ to 58% of upregulated and $\sim 76\%$ to 91% of downregulated genes following BRD32048 exposure were also up- or downregulated following shRNA-mediated knockdown of ETV1. This degree of overlap was highly significant for both upregulated ($P = 4.0 \times 10^{-20}$ and $P = 4.9 \times 10^{-25}$ for the 2 shRNA signatures) and downregulated ($P = 8.9 \times 10^{-34}$ and $P = 2.8 \times 10^{-138}$) genes (Fig. 2B and C). The overlap

remained highly significant (upregulated $P = 5.4 \times 10^{-13}$ and downregulated $P = 2 \times 10^{-39}$) when the 2 shETV1 signatures were merged and intersected with both compound signatures (Supplementary Fig. S4D), suggesting that BRD32048 may modulate the ETV1-dependent signature.

From the downregulated genes common to these 4 sets, we selected 8 genes that harbor multiple potential ETS binding sites in their promoter region and tested their expression following shETV1 or BRD32048 treatment. Quantitative RT-PCR results confirmed the microarray data, indicating comparable reductions in expression levels (Supplemental Fig. S4E). In contrast, similar experiments performed in the SK-MEL-28 melanoma cell line

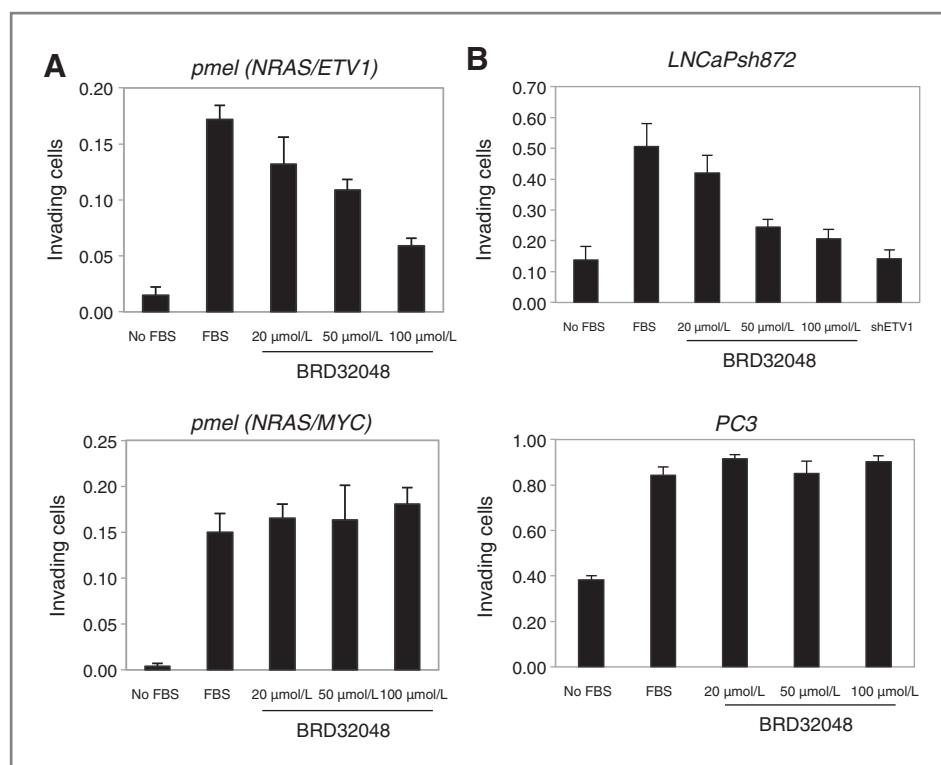


Figure 3. Effects of BRD2048 on tumor cell invasion. A, invasion of primary melanocytes, coexpressing NRAS^{G12D} with either ETV1 or MYC, was measured in invasion chambers after 24 hours in the presence of DMSO or BRD32048 at the indicated concentrations. B, invasion of LNCaP (shETV1-872) and PC3 cells was measured as indicated above. LNCaP cells were also treated with doxycycline for 4 days to express the shETV1-872.

did not yield any overlap between signatures obtained following shRNA knockdown of ETV1 (shETV1-3 and shETV1-5) and exposure of the cells to BRD32048 (Fig. 2D and E). ETV1 knockdown was confirmed by quantitative RT-PCR and Western blot analysis (Supplementary Fig. S4A and S4B). These results suggest that the effects of this compound may be influenced by genetic or lineage factors.

BRD32048 inhibits invasion of ETV1-dependent cell lines

We next wished to determine whether BRD32048 might modulate a tumor cell phenotype that is governed by ETV1 activity. Toward this end, ETV1 silencing can inhibit invasion or survival of some ETV1-dependent cancer cell lines (10, 44). We generated an isogenic system where primary melanocytes expressing NRAS^{G12D} were infected with either ETV1 or MYC (Supplementary Fig. S5A). These cell lines were assessed using an established collagen-based invasion assay (35). Ectopic expression of ETV1 in primary melanocytes expressing constitutive active NRAS^{G12D} significantly stimulates the invasive potential of these cells (Supplementary Fig. S5B). Treatment with BRD32048 for 24 hours inhibited invasion of cells expressing ETV1 in a dose-dependent manner, but not those expressing MYC (Fig. 3A). In contrast, we observed no inhibitory effects on the invasive phenotype of primary melanocytes expressing mutant NRAS only (Supplementary Fig. S5C), suggesting that the inhibitory effects involve an ETV1 cellular context. LNCaP cells were inhibited

in a concentration-dependent manner, with the highest concentration yielding comparable potency as with ETV1 knockdown (Fig. 3B). These results are reminiscent of prior studies showing that the invasive phenotype of LNCaP cells can be suppressed by silencing of ETV1 (44). In contrast, the invasion phenotype of PC3 cell line (which lack ETS factor rearrangements) was insensitive to compound treatment, likely because the invasive phenotype of PC3 cell line does not seem to be dependent on ETV1 (Supplementary Fig. S5D). Interestingly, 501mel cells, which have been shown previously to be ETV1-dependent (10) also showed suppressed invasive capacity following BRD32048 exposure, whereas SK-MEL-28 cells were unaffected (Supplementary Fig. S5E). The lack of effect of BRD32048 on SK-MEL-28 invasion is consistent with the observation that BRD32048 also did not inhibit the ETV1 signature in this cell line. The inhibitory effects of BRD32048 on the invasion phenotype of sensitive cell lines did not result from a global impairment of cell viability, because the cell lines used in the invasion assay showed no diminution of proliferative potential more than 4 days in the presence of 20, 50, and 100 μ mol/L BRD32048 compared with untreated controls (Supplementary Fig. S5F). Collectively, these results suggest that BRD32048 may inhibit a tumorigenic phenotype linked to ETV1 function.

BRD32048 inhibits ETV1 acetylation and promotes its degradation

To begin to explore the mechanism by which BRD32048 might perturb ETV1, we sought to determine its effect on

ETV1 protein function. We first assessed DNA-binding capacity (45) in the absence or presence of BRD32048 by performing oligonucleotide pull-down assays. Here, biotin-labeled oligonucleotides containing ETS binding sites were used to precipitate ETV1 from lysates of HEK 293T or LNCaP cells that overexpressed Flag-HA-tagged ETV1. BRD32048 had no effect on ETV1 pull-down in this assay, even at 100 $\mu\text{mol/L}$ concentrations (Supplementary Fig. S6A). In contrast, ETV1 pull-down was largely abrogated by excess unlabeled oligonucleotide, suggesting that the oligo-bound ETV1 may represent a relatively specific interaction. These results implied that BRD32048 might perturb ETV1 function in a DNA binding-independent manner, although a possible role for off-target compound effects could not be excluded completely.

We next sought to ascertain whether BRD32048 might alter the stability of ETV1 protein. To test this, we performed time course experiments to monitor the effects of the compound on exogenous Flag-HA ETV1 protein levels in the absence or presence of BRD32048. In the presence of cycloheximide (CHX), which blocks protein synthesis, the half-life of ETV1 was markedly reduced following pretreatment of either LNCaP or 501mel cells with BRD32048 for 24 hours. In contrast, BRD32048 did not affect ETV1 stability in SK-MEL-28 cells; this observation accords with the lack of BRD32048 effect on either the ETV1 gene expression signature or the invasion phenotype in these cells (Fig. 4A). The BRD32048-induced instability of exogenous ETV1 is also valid for endogenous ETV1 in 501mel and LNCaP cells following overnight treatment with BRD32048 (Supplementary Fig. S6B). This result suggested that BRD32048 might promote degradation of ETV1 in some but not all cellular contexts.

Previous studies suggest that ETV1 stability is enabled through acetylation of lysines situated at residues 33 and 116 (46). To determine if BRD32048 might alter ETV1 acetylation, we expressed Flag-HA-tagged ETV1 in our cell line panel, performed immunoprecipitations of ETV1 using an anti-Flag antibody, and examined its acetylation status by immunoblotting. ETV1 acetylation was readily detected following anti-Flag immunoprecipitation in LNCaP and 501mel cells (Fig. 4B). In contrast, no acetylation was observed in PC-3 cells or SK-MEL-28 cells, even after overexpression of exogenous p300 (Supplementary Fig. S6C). Interestingly, the ETV1 acetylation status was substantially reduced in both LNCaP and 501mel cells following 24 hours of pretreatment with 50 $\mu\text{mol/L}$ BRD32048, which was consistent with the reduction in ETV1 stability induced by this compound (Fig. 4B). Together, these results raised the possibility that BRD32048 binds and inhibits ETV1 function by reducing its acetylation and stability, thereby promoting cell context-dependent protein degradation.

Because various acetyltransferases are known to acetylate ETV1 (46), we sought to determine if the loss of acetylation conferred by BRD32048 in certain cell contexts might be linked to the activity of a particular HAT protein. To test this, we coexpressed ETV1 together with either

p300 or P/CAF in HEK293T cells in the absence or presence of 50 $\mu\text{mol/L}$ BRD32048. In this cell system, ectopic expression of both p300 and P/CAF induced ETV1 acetylation, as measured by Flag-immunoprecipitation followed by immunoblotting with the anti-acetyl antibody (Fig. 4C). However, only p300-dependent acetylation was inhibited by BRD32048 in this setting (Fig. 4C). In addition, shRNA-mediated knockdown of p300 protein reduced ETV1 protein levels in LNCaP and 501mel cells (Fig. 4D).

Previous studies have shown that p300 acetylates ETV1 at residues K33 and K116, and that these residues may also regulate ETV1 protein stability (46). Therefore, we reasoned that overexpression of an acetylation-deficient ETV1 mutant might counteract the inhibitory effects of BRD32048 towards this protein. We therefore generated a mutant form of ETV1 (K33R/K116R), which can no longer be acetylated by p300 (ref. 46; Supplementary Fig. S6D). Addition of BRD32048 to ETV1 (K33R/K116R) expressing cells had no effect on invasion (Supplementary Fig. S6E and S6F), in contrast to the effects of BRD32048 in cells overexpressing wild-type ETV1. Collectively, these findings suggest that BRD32048 may reduce p300-dependent ETV1 acetylation, thereby decreasing its stability in a context-dependent manner.

Discussion

Although many transcription factors play important roles in carcinogenesis and tumor progression, this class of proteins is traditionally considered poorly "druggable" by conventional means. Our results suggest that SMM screening may provide one approach through which to discover chemical probes that modulate the function of these and perhaps other "undruggable" proteins. Although we interrogated only 45,000 printed compounds, the SMM platform could easily be scaled to accommodate 100,000s of compounds in the future.

For our SMM screens, we utilized cell lysates that contained epitope-tagged ETV1. This approach may offer several advantages compared with the use of purified protein, as described previously (47). First, the use of cell lysates allows the protein of interest to be expressed in an appropriate cell context; for example, mammalian cells instead of bacterial or insect cells. This may allow the protein to undergo physiologically relevant posttranslational modifications that may affect its 3-dimensional structure and therefore its available binding surface. Second, lysates may retain multiprotein complexes that affect the conformation or avidity of the query protein. Third, preparation of cell lysates may offer technical advantages over protein purification, which may require extensive optimization to preserve protein folding and activity. Despite these potential advantages, it is often still necessary to utilize purified protein for subsequent validation steps, such as SPR-based binding studies, as performed here. Also, the use of lysates may carry an increased risk of false positives during the primary screen because of binding to other members of multiprotein complexes or

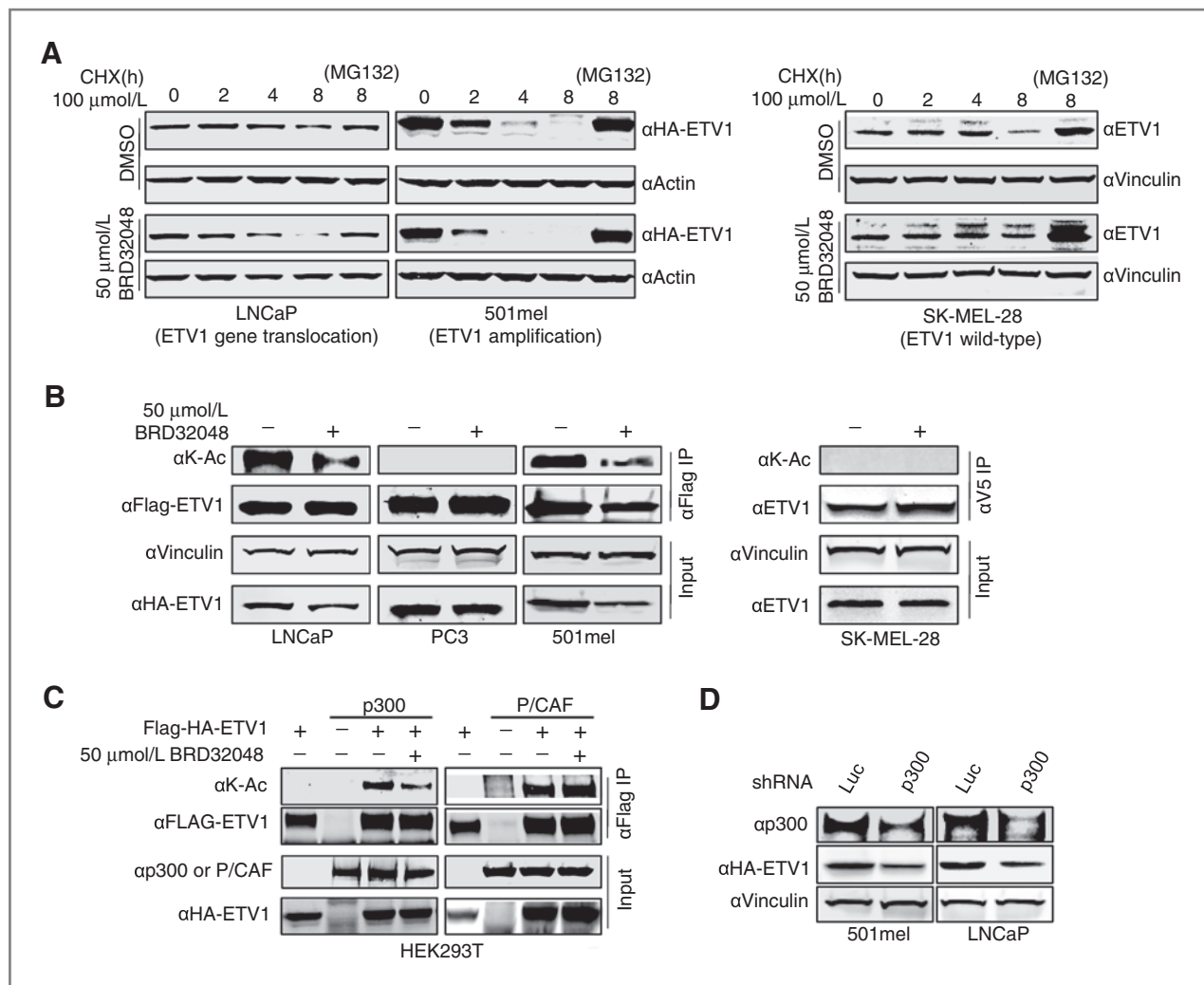


Figure 4. Effects of BRD32048 on ETV1 stability and acetylation. **A**, LNCaP and 501mel cells expressing Flag-HA-ETV1 and SK-MEL-28 expressing V5-ETV1 were pretreated (16 hours) with BRD32048 (50 μ mol/L) and subjected to a cycloheximide (100 μ mol/L) time course. ETV1 levels were evaluated at the indicated time points by immunoblotting. The proteasome inhibitor MG132 (10 μ mol/L) was used as a control. Actin and Vinculin were blotted for loading control. **B**, LNCaP, PC3, and 501mel cells expressing FLAG-HA-ETV1 or SK-MEL-28 expressing V5-ETV1 were pretreated (16 hours) with 50 μ mol/L of BRD32048. ETV1 immunoprecipitations were performed, and the resulting protein was probed with an antibody recognizing acetylated lysine (α K-Ac). Vinculin was probed as loading control. **C**, HEK293T cells coexpressing Flag-HA-ETV1 and either p300 or P/CAF were pretreated (16 hours) with 50 μ mol/L of BRD32048. Precipitated ETV1 was probed with anti-lysine-acetyl antibody. **D**, LNCaP and 501mel cells were infected with lentivirus expressing a p300 or luciferase shRNA (72 hours). Thereafter, the cells were transfected with Flag-HA-ETV1. After 48 hours, immunoblots were performed using antibodies directed against p300, HA-tag, or vinculin (control).

nonspecific interacting proteins. In the future, multiple SMM screens could be conducted in parallel using various alternative lysate preparations; for example, by expressing distinct epitope-tagged proteins in several cellular contexts before harvest. Here, small molecule "hits" identified in multiple screens could be prioritized for validation. The use of nuclear extracts instead of total protein lysates may also offer advantages in SMM screens that interrogate transcription factors.

Several lines of evidence support the premise that BRD32048 may alter the cellular function of ETV1 through direct binding. First, the SPR analysis indicates that BRD32048 can bind purified ETV1, albeit at micromolar

concentrations. In addition, a BRD32048 affinity resin is capable of precipitating endogenous ETV1 from cell lysates. Second, BRD32048 modulates a gene expression signature linked to ETV1 activity in cancer cell lines known to harbor an ETV1 dependency. The gene expression signature is directly linked to the availability and function of ETV1 protein. Although BRD32048 only marginally decreased ETV1 mRNA, it dramatically reduces ETV1 protein levels in certain cellular contexts, resembling the effects of shETV1. This may explain the overlapping mRNA signature between these 2 conditions. Third, BRD32048 exposure results in decreased ETV1 acetylation in the same cancer cell lines in which it

modulates the ETV1 signature and inhibits their invasion. Our data demonstrate that BRD32048 directly modulates the ETV1 protein stability, leading to a significant decrease in the amount of ETV1 molecules available to carry out the oncogenic functions of ETV1.

However, the exact location within the ETV1 protein to which BRD32048 binds remains unclear. One possibility is that the compound blocks K33 because P/CAF-dependent acetylation remains unaffected. Another possibility is that BRD32048 is directly interfering with a cofactor interaction or perhaps p300. The investigation of differential binding of ETV1 to its interaction partners in the presence or absence of BRD32048 may require structure-activity relationship (SAR) studies to identify derivatives that bind ETV1 with much higher affinity *in vitro*. Such studies would certainly aid understanding its specificity toward other cellular proteins, enabling quantitative target identification experiments involving mass spectrometry (48), as well as improve its *in vivo* potency. In the future, these avenues will likely be needed to develop molecules such as BRD32048 into mature chemical probes that explore biologic processes and possible therapeutic avenues linked to oncogenic transcription factors.

The observation that BRD32048 exposure may destabilize ETV1 by reducing its acetylation may highlight an alternative approach to therapeutic modulation of certain transcription factors that involves blocking vital post-translational modifications. In contrast to the transcription factors themselves, protein acetyltransferases may prove amenable to more conventional small-molecule discovery approaches. Toward this end, HATs are well-known transcriptional coactivators, and several HAT inhibitor tool compounds have been developed (49). Moreover, several previous reports have found that multiple ETS transcription factors including ETV1 can be regulated by acetylation in general and by p300 HAT activity in particular (46, 50). Thus far, however, few HAT inhibitors have entered clinical development. Additional studies of HAT inhibitors that exhibit selectivity for p300 may provide additional insights into the possible efficacy of such approaches against cancer cells that show dependence on ETV1 or other ETS factors for viability or tumor progression.

In summary, this study used an SMM screen to identify a compound capable of binding and inhibiting ETV1. The results may endorse a general approach to the discovery

of chemical probes that modulate transcription factors and other currently "undruggable" oncoproteins. Such studies may pave the way for future systematic efforts with important implications for chemical biology and therapeutic discovery.

Disclosure of Potential Conflicts of Interest

L.A. Garraway has a commercial research grant from Novartis; has ownership interest (including patents) in Foundation Medicine; and is a consultant/advisory board member for Novartis, Boehringer Ingelheim, Foundation Medicine, and Millenium. No potential conflicts of interest were disclosed by the other authors.

Disclaimer

The content of this publication does not necessarily reflect the views or policies of the Department of Health and Human Services, nor does mention of trade names, commercial products, or organizations imply endorsement by the U.S. Government.

Authors' Contributions

Conception and design: M.S. Pop, C. Zhong, D.S. Daniels, A.N. Koehler, L.A. Garraway

Development of methodology: M.S. Pop, N. Stransky, E.C. Hartman, C. Zhong, A.N. Koehler, L.A. Garraway

Acquisition of data (provided animals, acquired and managed patients, provided facilities, etc.): C. Zhong, E.K. Culyba, F. Lin, R. Pagliarini, L. Ronco, L.A. Garraway

Analysis and interpretation of data (e.g., statistical analysis, biostatistics, computational analysis): M.S. Pop, N. Stransky, J.-P. Theurillat, C. Zhong, F. Lin, R. Pagliarini, L. Ronco, A.N. Koehler, L.A. Garraway

Writing, review, and/or revision of the manuscript: M.S. Pop, N. Stransky, C. Zhong, D.S. Daniels, A.N. Koehler, L.A. Garraway

Administrative, technical, or material support (i.e., reporting or organizing data, constructing databases): M.S. Pop, C.W. Garvie, J.-P. Theurillat, T.A. Lewis, C. Zhong

Study supervision: M.S. Pop, C. Zhong, A.N. Koehler, L.A. Garraway

Acknowledgments

Plasmids expressing p300 and P/CAF were kindly provided by Dr. S.R. Grossman (VCU Massey Cancer Center, Richmond, VA).

Grant Support

The project was funded by the National Cancer Institute's Initiative for Chemical Genetics (ICG) under Contract No. N01-CO-12400, and the Cancer Target Discovery and Development (CTD²) Network, under RC2 CA148399 (A.N. Koehler), a New Innovator Award from the National Institutes of Health, and a Challenge Award from the Prostate Cancer Foundation (L.A. Garraway).

The costs of publication of this article were defrayed in part by the payment of page charges. This article must therefore be hereby marked *advertisement* in accordance with 18 U.S.C. Section 1734 solely to indicate this fact.

Received August 16, 2013; revised April 8, 2014; accepted April 9, 2014; published OnlineFirst April 15, 2014.

References

- Hopkins AL, Groom CR. The druggable genome. *Nat Rev Drug Discov* 2002;1:727-30.
- Boyd KE, Farnham PJ. Identification of target genes of oncogenic transcription factors. *Proc Soc Exp Biol Med* 1999;222:9-28.
- Darnell JE Jr. Transcription factors as targets for cancer therapy. *Nat Rev Cancer* 2002;2:740-9.
- Oh S, Shin S, Janknecht R. ETV1, 4 and 5: an oncogenic subfamily of ETS transcription factors. *Biochim Biophys Acta* 2012;1826:1-12.
- Janknecht R. EWS-ETS oncoproteins: the linchpins of Ewing tumors. *Gene* 2005;363:1-14.
- Tomlins SA, Rhodes DR, Perner S, Dhanasekaran SM, Mehra R, Sun XW, et al. Recurrent fusion of TMPRSS2 and ETS transcription factor genes in prostate cancer. *Science* 2005;310:644-8.
- Baca SC, Prandi D, Lawrence MS, Mosquera JM, Romanel A, Drier Y, et al. Punctuated evolution of prostate cancer genomes. *Cell* 2013;153:666-77.
- Tomlins SA, Laxman B, Dhanasekaran SM, Helgeson BE, Cao X, Morris DS, et al. Distinct classes of chromosomal rearrangements create oncogenic ETS gene fusions in prostate cancer. *Nature* 2007;448:595-9.

9. Hermans KG, van der Korput HA, van Marion R, van de Wijngaart DJ, Ziel-van der Made A, Dits NF, et al. Truncated ETV1, fused to novel tissue-specific genes, and full-length ETV1 in prostate cancer. *Cancer Res* 2008;68:7541–9.
10. Jane-Valbuena J, Widlund HR, Perner S, Johnson LA, Dibner AC, Lin WM, et al. An oncogenic role for ETV1 in melanoma. *Cancer Res* 2010;70:2075–84.
11. Chi P, Chen Y, Zhang L, Guo X, Wongvipat J, Shamu T, et al. ETV1 is a lineage survival factor that cooperates with KIT in gastrointestinal stromal tumours. *Nature* 2010;467:849–53.
12. Shin S, Kim TD, Jin F, van Deursen JM, Dehm SM, Tindall DJ, et al. Induction of prostatic intraepithelial neoplasia and modulation of androgen receptor by ETS variant 1/ETS-related protein 81. *Cancer Res* 2009;69:8102–10.
13. Baena E, Shao Z, Linn DE, Glass K, Hamblen MJ, Fujiwara Y, et al. ETV1 directs androgen metabolism and confers aggressive prostate cancer in targeted mice and patients. *Genes Dev* 2013;27:683–98.
14. Janknecht R. Regulation of the ER81 transcription factor and its coactivators by mitogen- and stress-activated protein kinase 1 (MSK1). *Oncogene* 2003;22:746–55.
15. Oh S, Shin S, Lightfoot SA, Janknecht R. 14-3-3 proteins modulate the ETS transcription factor ETV1 in prostate cancer. *Cancer Res* 2013;73:5110–9.
16. Goel A, Janknecht R. Concerted activation of ETS protein ER81 by p160 coactivators, the acetyltransferase p300 and the receptor tyrosine kinase HER2/Neu. *J Biol Chem* 2004;279:14909–16.
17. Bosc DG, Goueli BS, Janknecht R. HER2/Neu-mediated activation of the ETS transcription factor ER81 and its target gene MMP-1. *Oncogene* 2001;20:6215–24.
18. Fuchs B, Inwards CY, Janknecht R. Upregulation of the matrix metalloproteinase-1 gene by the Ewing's sarcoma associated EWS-ER81 and EWS-Fli-1 oncoproteins, c-Jun and p300. *FEBS Lett* 2003;553:104–8.
19. Vitari AC, Leong KG, Newton K, Yee C, O'Rourke K, Liu J, et al. COP1 is a tumour suppressor that causes degradation of ETS transcription factors. *Nature* 2011;474:403–6.
20. Baert JL, Monte D, Verreman K, Degerny C, Coutte L, de Launoit Y. The E3 ubiquitin ligase complex component COP1 regulates PEA3 group member stability and transcriptional activity. *Oncogene* 2010;29:1810–20.
21. Filippakopoulos P, Qi J, Picaud S, Shen Y, Smith WB, Fedorov O, et al. Selective inhibition of BET bromodomains. *Nature* 2010;468:1067–73.
22. Rahim S, Beauchamp EM, Kong Y, Brown ML, Toretsky JA, Uren A. YK-4-279 inhibits ERG and ETV1 mediated prostate cancer cell invasion. *PLoS ONE* 2011;6:e19343.
23. Barber-Rotenberg JS, Selvanathan SP, Kong Y, Erkizan HV, Snyder TM, Hong SP, et al. Single enantiomer of YK-4-279 demonstrates specificity in targeting the oncogene EWS-FLI1. *Oncotarget* 2012;3:172–82.
24. Clemons PA, Bodycombe NE, Carrinski HA, Wilson JA, Shamji AF, Wagner BK, et al. Small molecules of different origins have distinct distributions of structural complexity that correlate with protein-binding profiles. *Proc Natl Acad Sci U S A* 2010;107:18787–92.
25. Bradner JE, McPherson OM, Koehler AN. A method for the covalent capture and screening of diverse small molecules in a microarray format. *Nat Protoc* 2006;1:2344–52.
26. Bradner JE, McPherson OM, Mazitschek R, Barnes-Seeman D, Shen JP, Dhaliwal J, et al. A robust small-molecule microarray platform for screening cell lysates. *Chem Biol* 2006;13:493–504.
27. Miao H, Tallarico JA, Hayakawa H, Munger K, Duffner JL, Koehler AN, et al. Ring-opening and ring-closing reactions of a shikimic acid-derived substrate leading to diverse small molecules. *J Comb Chem* 2007;9:245–53.
28. Ng PY, Tang Y, Knosp WM, Stadler HS, Shaw JT. Synthesis of diverse lactam carboxamides leading to the discovery of a new transcription-factor inhibitor. *Angew Chem Int Ed Engl* 2007;46:5352–5.
29. Duffner JL, Clemons PA, Koehler AN. A pipeline for ligand discovery using small-molecule microarrays. *Curr Opin Chem Biol* 2007;11:74–82.
30. Petri Seiler K, Kuehn H, Pat Happ M, Decaprio D, Clemons PA. Using ChemBank to probe chemical biology. *Curr Protoc Bioinform* 2008; Chapter 14:Unit 14.5.
31. Dai M, Wang P, Boyd AD, Kostov G, Athey B, Jones EG, et al. Evolving gene/transcript definitions significantly alter the interpretation of GeneChip data. *Nucleic Acids Res* 2005;33:e175.
32. Irizarry RA, Hobbs B, Collin F, Beazer-Barclay YD, Antonellis KJ, Scherf U, et al. Exploration, normalization, and summaries of high density oligonucleotide array probe level data. *Biostatistics* 2003;4:249–64.
33. Bolstad BM, Irizarry RA, Astrand M, Speed TP. A comparison of normalization methods for high density oligonucleotide array data based on variance and bias. *Bioinformatics* 2003;19:185–93.
34. Wettenhall JM, Smyth GK. limmaGUI: a graphical user interface for linear modeling of microarray data. *Bioinformatics* 2004;20:3705–6.
35. Repesh LA. A new *in vitro* assay for quantitating tumor cell invasion. *Invasion Metastasis* 1989;9:192–208.
36. Miyazaki I, Simizu S, Okumura H, Takagi S, Osada H. A small-molecule inhibitor shows that pirin regulates migration of melanoma cells. *Nat Chem Biol* 2010;6:667–73.
37. Seiler KP, George GA, Happ MP, Bodycombe NE, Carrinski HA, Norton S, et al. ChemBank: a small-molecule screening and cheminformatics resource database. *Nucleic Acids Res* 2008;36:D351–9.
38. Yasumoto K, Yokoyama K, Shibata K, Tomita Y, Shibahara S. Microphthalmia-associated transcription factor as a regulator for melanocyte-specific transcription of the human tyrosinase gene. *Mol Cell Biol* 1994;14:8058–70.
39. Garraway LA, Widlund HR, Rubin MA, Getz G, Berger AJ, Ramaswamy S, et al. Integrative genomic analyses identify MITF as a lineage survival oncogene amplified in malignant melanoma. *Nature* 2005;436:117–22.
40. Gewald R, Grunwald C, Egerland U. Discovery of triazines as potent, selective and orally active PDE4 inhibitors. *Bioorg Med Chem Lett* 2013;23:4308–14.
41. Mui EJ, Schiehsler GA, Milhous WK, Hsu H, Roberts CW, Kirisits M, et al. Novel triazine JPC-2067-B inhibits *Toxoplasma gondii* *in vitro* and *in vivo*. *PLoS Negl Trop Dis* 2008;2:e190.
42. Venkatesan AM, Chen Z, dos Santos O, Dehnhardt C, Santos ED, Ayril-Kaloustian S, et al. PKI-179: an orally efficacious dual phosphatidylinositol-3-kinase (PI3K)/mammalian target of rapamycin (mTOR) inhibitor. *Bioorg Med Chem Lett* 2010;20:5869–73.
43. Wurz RP, Liu L, Yang K, Nishimura N, Bo Y, Pettus LH, et al. Synthesis and structure-activity relationships of dual PI3K/mTOR inhibitors based on a 4-amino-6-methyl-1,3,5-triazine sulfonamide scaffold. *Bioorg Med Chem Lett* 2012;22:5714–20.
44. Cai C, Hsieh CL, Omwancha J, Zheng Z, Chen SY, Baert JL, et al. ETV1 is a novel androgen receptor-regulated gene that mediates prostate cancer cell invasion. *Mol Endocrinol* 2007;21:1835–46.
45. Nhili R, Peixoto P, Depauw S, Flajollet S, Dezitter X, Munde MM, et al. Targeting the DNA-binding activity of the human ERG transcription factor using new heterocyclic dithiophene diamidines. *Nucleic Acids Res* 2013;41:125–38.
46. Goel A, Janknecht R. Acetylation-mediated transcriptional activation of the ETS protein ER81 by p300, P/CAF, and HER2/Neu. *Mol Cell Biol* 2003;23:6243–54.
47. Kemp MM, Weiwer M, Koehler AN. Unbiased binding assays for discovering small-molecule probes and drugs. *Bioorg Med Chem* 2012;20:1979–89.
48. Ong SE, Schenone M, Margolin AA, Li X, Do K, Doud MK, et al. Identifying the proteins to which small-molecule probes and drugs bind in cells. *Proc Natl Acad Sci U S A* 2009;106:4617–22.
49. Bowers EM, Yan G, Mukherjee C, Orry A, Wang L, Holbert MA, et al. Virtual ligand screening of the p300/CBP histone acetyltransferase: identification of a selective small molecule inhibitor. *Chem Biol* 2010;17:471–82.
50. Czuwara-Ladykowska J, Sementchenko VI, Watson DK, Trojanowska M. Ets1 is an effector of the transforming growth factor beta (TGF- β) signaling pathway and an antagonist of the profibrotic effects of TGF- β . *J Biol Chem* 2002;277:20399–408.

Molecular Cancer Therapeutics

A Small Molecule That Binds and Inhibits the ETV1 Transcription Factor Oncoprotein

Marius S. Pop, Nicolas Stransky, Colin W. Garvie, et al.

Mol Cancer Ther 2014;13:1492-1502. Published OnlineFirst April 15, 2014.

Updated version Access the most recent version of this article at:
doi:[10.1158/1535-7163.MCT-13-0689](https://doi.org/10.1158/1535-7163.MCT-13-0689)

Supplementary Material Access the most recent supplemental material at:
<http://mct.aacrjournals.org/content/suppl/2014/04/17/1535-7163.MCT-13-0689.DC1>

Cited articles This article cites 49 articles, 12 of which you can access for free at:
<http://mct.aacrjournals.org/content/13/6/1492.full#ref-list-1>

Citing articles This article has been cited by 6 HighWire-hosted articles. Access the articles at:
<http://mct.aacrjournals.org/content/13/6/1492.full#related-urls>

E-mail alerts [Sign up to receive free email-alerts](#) related to this article or journal.

Reprints and Subscriptions To order reprints of this article or to subscribe to the journal, contact the AACR Publications Department at pubs@aacr.org.

Permissions To request permission to re-use all or part of this article, use this link
<http://mct.aacrjournals.org/content/13/6/1492>.
Click on "Request Permissions" which will take you to the Copyright Clearance Center's (CCC) Rightslink site.